Effects of Differential Pavement Friction on the Response of Cars in Skidding Maneuvers

GORDON F. HAYHOE AND JOHN J. HENRY

A simulation study of the skidding behavior of cars in plane motion on surfaces with differential friction is described. Vehicle drift angle and forward velocity are taken as indicators of the difficulty a driver will experience in regaining control of the vehicle, and maintaining it within the specified roadway boundaries, should the driver release the brakes at some point during a locked-wheel skidding maneuver. Boundaries of safe vehicle operation are given as functions of roadway coefficients of friction and the length of the roadway where differential friction exists.

Areas of nonuniform tire-pavement friction across a pavement surface can arise from a number of causes, such as patching, resurfacing of worn wheel tracks, and application of marking materials for delineation. A car passing from the normal traveled way to a hard shoulder will also experience different coefficients of friction at the tires on either side of the vehicle, as will a car that has differentially worn tires.

Differential friction can either exacerbate the effects of an emergency maneuver (a locked-wheel skid, for example) or precipitate an emergency during an otherwise normal maneuver (due to the unexpected locking of a wheel, for example). The purpose of this study was to set limits on the tolerable differential friction for the safe operation of cars. Computer simulations were used to study vehicle behavior under a set of prescribed conditions.

Nonskidding maneuvers, or those in which independent locking of one or more of the wheels of the vehicle occurs, usually involve complex interaction between the driver and the vehicle. In these cases, an analytic examination of the vehicle motion is not possible because realistic models of driver behavior have not been formulated. However, a common response of car drivers to an emergency is simply to lock the wheels of the car. As will be shown later, a full, locked-wheel skid on a surface with differential friction is not much more hazardous than one on a surface with uniform friction. But if, on a surface with differential friction, the driver releases the brakes before the vehicle comes to rest, the ensuing maneuver may be extremely hazardous.

Therefore, the following maneuver was chosen to assess the hazard associated with driving a car on a differential-friction surface. The vehicle is skidding on a uniform surface and then passes onto a section of roadway where the coefficients of friction are different for the tires on either side of the vehicle. Steer angle is initially at zero degrees and is held constant during the maneuver. Two parameters describing the yaw motion of the vehicle are monitored throughout the locked-wheel skidding maneuver and, if either exceeds a certain level, it is assumed that the driver will not be able to regain control should he or she release the brakes. The primary objective of the study was then to establish boundaries of safe operation in terms of the two coefficients of friction: the length along the pavement for which the differential friction exists and the initial vehicle speed. Figure 1 shows the assumed roadway conditions for the maneuver.

In this paper, the parameter that describes the ability of a surface to provide frictional forces is referred to as "coefficient of friction" rather than "skid number". This nomenclature emphasizes the fact that the results are given in terms of vehicle-tire/pavement properties and not in terms of pavement properties as described by a locked-wheel skid number (SN_{40}) measured according to American Society for Testing and Materials (ASTM) test method E274 (1). Skid numbers are used for ranking assumed uniform sections of pavement in terms of their "skid resistance" and are not intended to describe the true coefficient of friction experienced by a typical highway vehicle. In contrast, the present work aims at assessing the relative hazard associated with different levels of suddenly changing friction on a pavement surface. Estimates of the true coefficients of the pavement surfaces are therefore required.

VEHICLE RESPONSE DURING A SKIDDING MANEUVER

In a pure skidding maneuver, the presence of differential friction on the pavement causes vehicle yaw and an increase in stopping distance that depends on the change in effective total friction. If the vehicle is maintained in a skid (i.e., the wheels are kept locked), the trajectory of the center of gravity is very close to a straight line; the only difference in vehicle response on pavement surfaces with and without differential friction is the increased stopping distance and vehicle yaw. In this case, the procedures currently used to determine acceptable skid resistance can be applied by estimating the "effective" coefficient of friction and by allowing for the increased hazard of an increase in effective vehicle width as the vehicle rotates. The effective friction and additional hazard would have to be determined for each individual site, which would make a general criterion for acceptability difficult to formulate. However, the full skidding maneuver is a special case of the general maneuver in which a driver locks the wheels, the vehicle skids some distance, and the driver then releases the brakes. If the coefficient of friction is uniform over the pavement surface, the vehicle will not rotate during the maneuver and the driver can reapply the brakes while maintaining steering control. If the friction is nonuniform, the vehicle will rotate during the skid and, on release of the brakes, will travel in a direction different from the original. If the yaw angle is great enough, the driver may not have steering control.

Figure 1. Pavement surface with differential friction as idealized in simulation study.

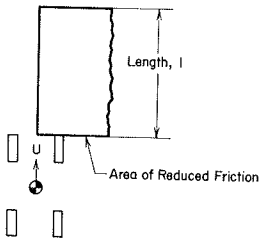

Figure 2. Vehicle axis system and vehicle parameters.

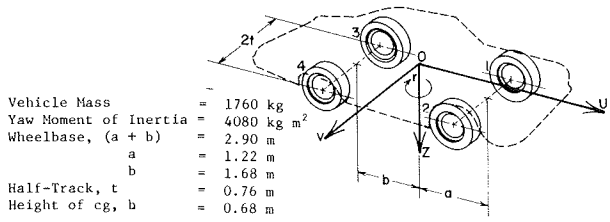

Figure 3. Simulation tire model results for free rolling and locked-wheel sliding.

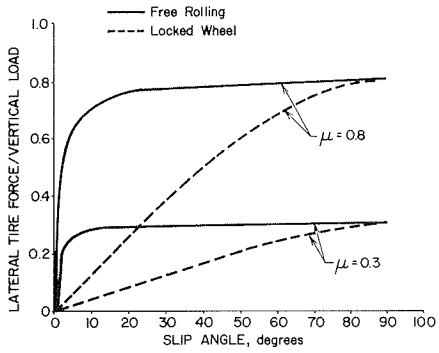

Figure 4. Variables defining kinematics of four-wheeled vehicle motion.

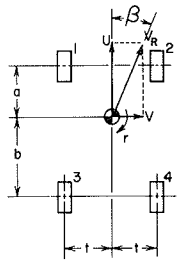

U = Forward Velocity

V = Lateral Velocity

V_r = Resultant Velocity = $\sqrt{U^2 + V^2}$

β = Drift Angle = Arctan (V/U)

r = Yaw Rate = Angular Velocity about a Vertical Axis through the cg

Tire Slip Angles (α):

$\alpha_1 = \text{Arctan}\left(\frac{V + a.r}{U + t.r}\right)$

$\alpha_2 = \text{Arctan}\left(\frac{V + a.r}{U - t.r}\right)$

$\alpha_3 = \text{Arctan}\left(\frac{V - b.r}{U + t.r}\right)$

$\alpha_4 = \text{Arctan}\left(\frac{V - b.r}{U - t.r}\right)$

SIMULATION MODEL

The effect of differential friction on safe car operation was studied by means of a digital computer simulation in which the vehicle was given an initial velocity, direction, and position relative to the nonuniform portion of the pavement. By an extension of the argument given in the previous section, the particular pavement configuration was considered to be unsafe if (a) at some point during the skid the heading of the vehicle changed by more than 20° from its original direction or (b) at some point during the skid the product of drift angle (body sideslip angle) and forward velocity exceeded a value of 3.66 m/s (where drift angle is defined as the angle between the longitudinal axis of the vehicle and the resultant velocity vector at the center of gravity, as shown later in Figure 4).

The first condition expresses the fact that the driver has no steering control over the vehicle at large yaw angles and that the vehicle will not continue to travel in the original direction when the brakes are released. The second condition expresses the fact that, after the brakes are released, the vehicle is likely to travel off the highway before the driver has an opportunity to take control and change the vehicle heading.

The simulation model has three degrees of freedom: forward velocity (U), lateral velocity (V), and yaw velocity (r). Figure 2 shows the variables and the general layout of the model. The vehicle model has four wheels; the tire forces at each wheel are found by using a tire model (2) that calculates the forces under all conditions of lateral and longitudinal slip. Vehicle suspension effects, such as roll steer and compliance steer, are neglected, although load transfer is included through a quasi-static analysis.

DETERMINATION OF CRITERIA FOR SAFE OPERATION

Vehicle control is, in general, a process in which the driver turns the steering wheel to modify the lateral forces generated at the front tires of the vehicle. Whether the front tire forces can be changed by small steering motions is therefore of fundamental importance to efficient control and, by extension, so is the shape of the lateral tire force characteristic. Figure 3 shows plots of lateral tire force versus slip angle for free rolling and locked-wheel sliding at coefficients of friction of 0.8 and 0.3. [Slip angle is the angle between the diametral plane of the wheel and the resultant velocity vector (in the horizontal plane) of the wheel axle.] The plots were taken from tire model results with the coefficient of friction constant with speed. But, since coefficient of friction generally decreases with increasing speed, experimental free-rolling lateral tire force characteristic curves typically show a peak in lateral force at a slip angle between 10° and 20°. This somewhat unrealistic aspect of the plots does not affect the following discussion; the important characteristic is that, for a free-rolling tire, the slope of the curves at large slip angles (greater than about 5°) is small compared with the slope at small slip angles.

Consider a vehicle sliding with locked wheels on a surface that has a uniform coefficient of friction at a given drift angle (β), yaw rate (r), and sliding velocity (V_r), as shown in Figure 4. [In Figures 4-7, a = locked-wheel sliding on a split-coefficient surface, b = locked-wheel sliding on a uniform-coefficient surface (y = 0.6), and c = free-rolling wheels on a uniform-coefficient surface (y = 0.6) and brake release is at 1.5 s).] Under these conditions, the vehicle will rotate about its center of gravity and travel in the direction of the V_r vector at decreasing rates until it stops. However, if the brakes are released during the maneuver, the lateral tire forces will rapidly attain the values given by the free-rolling tire force characteristic curve, disturbing the vehicle from its straight-line motion.

With free-rolling wheels, the net yaw moment about the center of gravity of the vehicle is given by the expression

$$M_z = a \cdot Y_f - b \cdot Y_r \quad (1)$$

where Y_f and Y_r are front and rear lateral tire

forces, respectively, as determined from the characteristic curves (Figure 3). Therefore,

$$M_z = a \cdot [f(\alpha_1) + f(\alpha_2)] - b \cdot [F(\alpha_3) + F(\alpha_4)] \approx a \cdot f[(V + a \cdot r)/U] - b \cdot F[(V - a \cdot r)/U] \quad (2)$$

For the vehicle-pavement configuration shown in Figure 1, yaw rate (r) will be negative and lateral velocity (V) will, in general, be positive during the maneuver. Negative slip angles give positive side forces, and the net yaw moment will therefore be positive for both locked and free-rolling wheels.

If, during the skidding maneuver, drift angle is small, the lateral velocity will be of the same order of magnitude as the a • r and b • r terms in the slip-angle expressions. The locked-wheel side forces will also be small. When the brakes are released, the lateral tire forces will increase and generate a large positive yaw moment that will decrease yaw rate and stabilize the vehicle motion at some final heading angle (to the original direction of V_r). When the front tire force is on the part of the tire curve that has high slope (small α_f), it is clear that vehicle yaw rate will always go to zero when there is no control action by the driver and that the front tire force can easily be changed by the driver if he or she turns the steering wheel.

At large drift angles, lateral velocity (V) will be the dominant term in the slip-angle expressions except when yaw rate is unreasonably large. When the brakes are released, the magnitude of the lateral tire forces at the front and rear will be determined almost wholly by the drift angle and will therefore give approximately equal and opposite yaw moments about the center of gravity while both front and rear tires are operating at large slip angles. Modification of the slip angles by the yaw-rate terms will have little effect because of the small slope at large slip angles. The result is that the vehicle will maintain an approximately constant yaw rate while moving laterally under the influence of the large lateral tire forces.

Figures 5, 6, and 7 show yaw-rate, drift-angle, and heading-angle responses for lengths of differential friction of 3, 12, and 24 m, where the brakes are released 1.5 s after the start of the maneuver (drift angle is positive for negative yaw rate and heading angle). The pavement coefficients of friction are 0.6 and 0.2. [Heading angle is defined as the angle through which the vehicle rotates from the start of the maneuver (t = 0) to time t (as shown later in Figure 9). The different scales on the vertical axes of the three plots should be noted.]

In Figure 5, yaw velocity, drift angle, and heading angle increase while the vehicle is sliding on the split-coefficient surface. Yaw rate then decreases when the vehicle is sliding on the uniform-coefficient surface, while drift and heading angle continue to increase. When the brakes are released and the wheels are allowed to turn freely, drift angle is 5.5°; this small value causes the yaw rate and the drift angle to decrease rapidly to zero through the mechanism described previously. The heading angle goes to a constant value, and the final vehicle trajectory is a straight line at the steady-state heading angle. Full steering control is available to the driver as soon as the brakes are released.

In Figure 6, the vehicle motion follows the same pattern as in Figure 5 until brake release, except that the three variables reach larger values because of the increased length of time on the split-coefficient surface. When the brakes are released, the drift angle has a value of 20° and the yaw rate decreases much more slowly than in Figure 5. The yaw rate does not begin to decrease at a significant rate until the drift angle has become less than 10°, 2 s after brake release. To gain sufficient steering control to stabilize the vehicle, the driver must reduce the front-wheel slip angle to less than 5°. For a drift angle of 20°, the driver must therefore turn the steering wheel through at least 300° (assuming a steering gear ratio of 20:1). The maximum steering-wheel rotation rate for a typical driver is approximately 400°/s (3). Thus, if driver

Figure 5. Yaw rate, heading angle, and drift angle response of four-wheeled vehicle when brakes are released during skidding maneuver across 3-m-long split-coefficient surface.

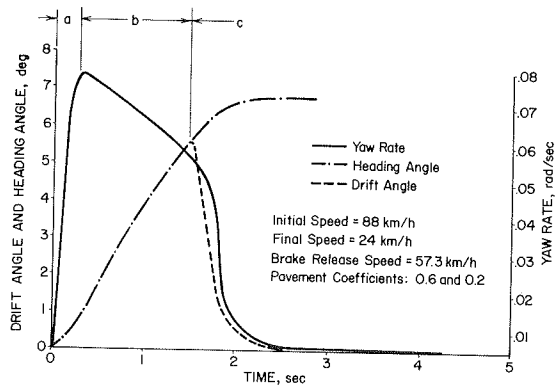

Figure 6. Yaw rate, heading angle, and drift angle response of four-wheeled vehicle when brakes are released during skidding maneuver across 12-m-long section of split-coefficient surface.

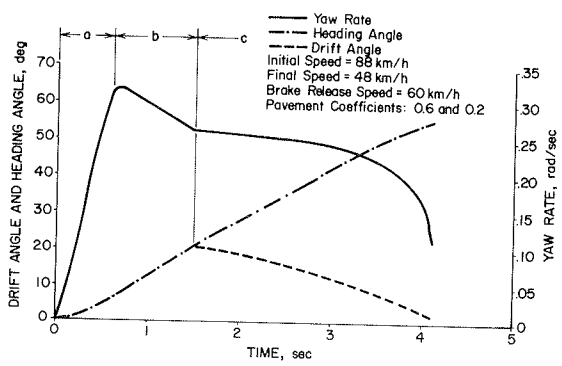

Figure 7. Yaw rate, heading angle, and drift angle response of four-wheeled vehicle when brakes are released during skidding maneuver across 24-m-long section of split-coefficient surface.

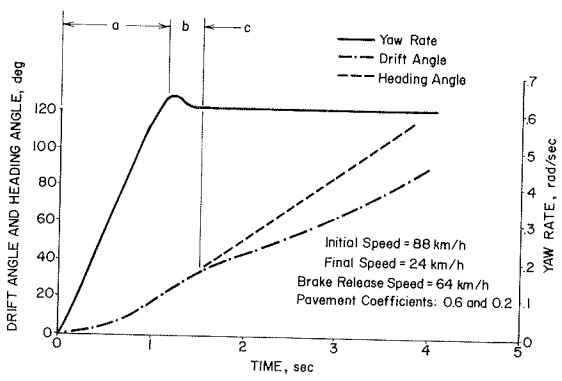

Figure 8. Lateral deviation during skidding maneuvers when brakes are released 1.5 s after initiation of skid.

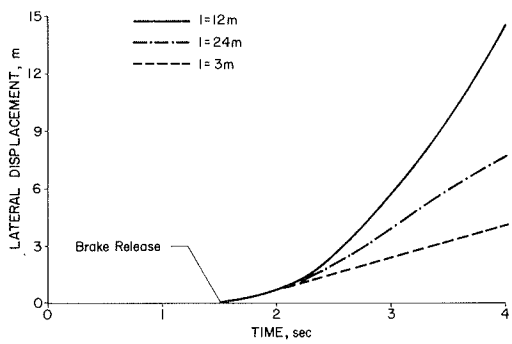

Figure 9. Lateral displacement of vehicle traveling obliquely across a road at steady forward speed.

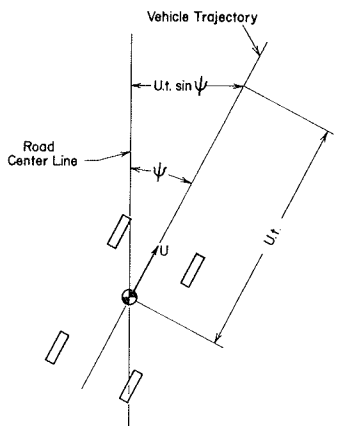

response time is ignored, about 1 s will pass after brake release before the driver can begin to significantly influence the behavior of the vehicle. This analysis also assumes that the driver makes the correct response.

In Figure 7, drift angle is 33° when the brakes are released, and the vehicle continues to spin at a constant yaw rate through the remainder of the maneuver. The drift angle also continues to increase in this case because the increase in lateral velocity due to vehicle rotation exceeds the decrease due to lateral acceleration. It is clear that the vehicle motion is completely unstable and that the driver cannot influence vehicle behavior during either the locked-wheel or the free-rolling wheel phases by turning the steering wheel.

Figure 8 shows the lateral deviation of the vehicle perpendicular to the initial heading. Lateral deviation in the last two cases (l = 12 m and l = 24 m) is in excess of 3 m 1.75 s after brake release. However, driver control action may be expected to reduce this for l = 12 m.

From these results, and from the general description already given of vehicle response in skidding maneuvers, it is clear that releasing the brakes is the most hazardous response that a driver can make in a skidding maneuver where all four wheels are locked and the vehicle is sideslipping at a large drift angle. Once the brakes are released, the ability of the driver to regain control before colliding with another vehicle or with a roadside obstacle depends in the first case on the drift angle of the vehicle. Consequently, an unsafe condition would exist if, at any point during either of the simulated locked-wheel skidding maneuvers, the vehicle drift angle exceeded a value of 20°. This value was chosen partly because it represented the transition between a decrease or an increase in the drift angle after brake release in the maneuvers used to produce the results shown in Figures 5-7. A further reason was that 20° is an upper limit on the angle through which a driver can reasonably be expected to turn the wheels of a car in 1 s. A longer delay will probably result in the vehicle passing into a potential collision zone before the driver can regain full control.

The 20° drift-angle limit is independent of speed, but experience suggests that vehicle control becomes more difficult as speed increases. A full explanation of this effect cannot be given, although important to the present work is the fact that a vehicle traveling at a nonzero heading angle will travel sideways, relative to the center of the road, at a rate in direct proportion to forward speed times the sine of the heading angle ($U \cdot \sin \psi$), as demonstrated in Figure 9. The parameter $U \cdot \sin \psi$ is given in terms of steady-state forward speed and heading angle with free-rolling wheels, but the desired parameter should be expressed in terms of vehicle variable values measured during a locked-wheel skid. The substitution of drift angle (β) for heading angle is later shown to be a reasonable transformation. In addition, if $U \cdot \sin \beta$ is taken as a limiting factor in vehicle response, it will be the deciding factor only when drift angle is less than 20°. The expression may therefore be simplified to $U \cdot \beta$ with little change in the numerical values.

An upper limit of 3.66 m/s was placed on $U \cdot \beta$; if this value was exceeded during a simulated maneuver, a hazard was considered to exist (U is in meters per second and β is in radians). The choice of $U \cdot \beta = 3.66$ m assumes that (a) the vehicle must travel 3.66 m laterally to enter a potential collision zone, (b) the yaw rate reduces instantaneously to zero and the vehicle travels in the direction of its heading at brake release, and (c) the driver is allowed 1 s to regain control and steer the vehicle to a safe path. The third assumption is the most difficult to justify, since both driver response time and time to regain control must be taken into account. For example, if the driver makes no steering correction at all, he or she will exceed the 3.66-m allowed lateral displacement in 1 s. But if the driver begins steering action at, say, 0.5 s after brake release, the heading angle will decrease during the remaining time, thus effectively allowing more time to steer the vehicle to a safe path within the 3.66-m lateral displacement limit.

The allowance of just 1 s for the driver to respond and control the vehicle would probably be too short if the yaw rate did indeed reduce to zero instantaneously. But Figures 5-7 show that this assumption becomes less true as the drift angle at brake release increases. Figure 8 shows the effect on lateral displacement. For example, when l = 3 m, $U \cdot \beta = 1.55$ m at brake release and lateral displacement 1 s later is 1.43 m. Lateral displacement 1 s after brake release is therefore slightly overpredicted by $U \cdot \beta$. In contrast, $U \cdot \beta$ overpredicts lateral displacement by more than a factor of two when l = 12.2 m. Drift angle, heading angle, and $U \cdot \beta$ at brake release, and drift angle and lateral displacement 1 s after brake release, are shown in Figure 10.

The maximum allowable lateral deviation of 3.66 m was chosen to conform with work by Burns (4), where a vehicle is considered to have entered a potential collision zone when it moves from the center of a

Figure 10. Vehicle response at brake release and 1 s after brake release.

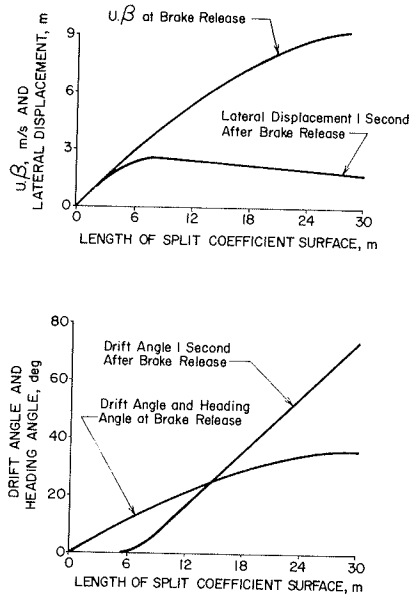

lane 3.66 m in width to the center of an adjacent lane also 3.66 m in width. The maximum allowable lateral deviation may be increased or decreased according to the width of the roadway.

Burns (4) also gives an experimental justification for some of the conclusions drawn from the simulation. He describes a series of experiments in which a professional driver locked the wheels of a car on a split-coefficient surface and then released the brakes after the car had rotated through a specified angle. Specific findings were that (a) a rotation in excess of 30° caused the vehicle to be completely uncontrollable; (b) the permissible angle of rotation at brake release, without loss of control, decreased as vehicle speed increased; and (c) the vehicle entered a potential collision zone after release of the brakes at a rotation of 10° and a vehicle speed of 80 km/h. These results are important because they are based on the only full-scale experimental data on vehicle loss of control on split-coefficient surfaces. However, the number of tests conducted was small, and the experienced driver's performance may not be typical of that of the general driving population confronted with an unexpected maneuver. Direct correlation of the simulation results with the experimental results therefore was not possible. [Zuk (5) gives a plot of a typical trajectory for a scale-model car sliding with locked wheels on a split-coefficient surface, but the effect of releasing the brakes is not considered.]

A study of vehicle-driver behavior after brake release by including a steering controller in the simulation was not attempted because none of the available models (6,7) accurately reproduced the behavior of a human driver, particularly in emergency maneuvers.

BOUNDARIES OF SAFE OPERATION

The simulation runs were made at an initial vehicle speed of 88 km/h. In most cases, either the U • β limit was exceeded before the drift-angle limit or neither of the two limits was exceeded. However, in some runs U • β reached a maximum value that was less than 3.66 while drift angle exceeded its limit at a relatively low speed. When this occurred, the maneuver was considered to be hazardous if drift angle exceeded 20° at a vehicle speed of 32 km/h or more. It should be noted that changing the vehicle parameters or the initial speed may reverse the order in which the parameters are exceeded, as will changing the specified safe limit for U • β or β.

Figures 11 and 12 show the maximum values of U • β attained during the simulation runs, plotted as a function of split-coefficient length at various combinations of coefficients of friction. The lengths where the curves cross the U • β = 3.66 line are shown in Figure 13. Also shown in Figure

Figure 11. Maximum U · β attained during locked-wheel skid on split-coefficient surface (initial vehicle speed = 88 km/h).

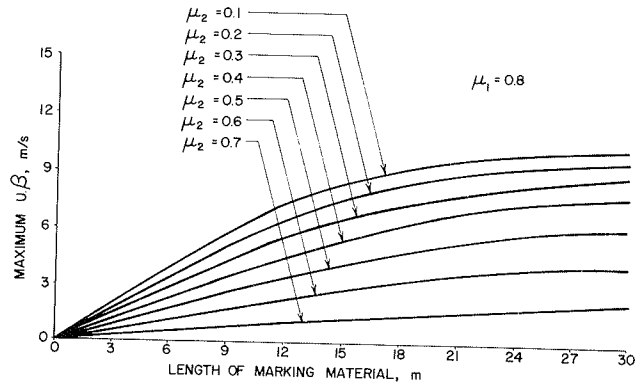

Figure 12. Maximum U · β attained (initial vehicle speed = 88 km/h).

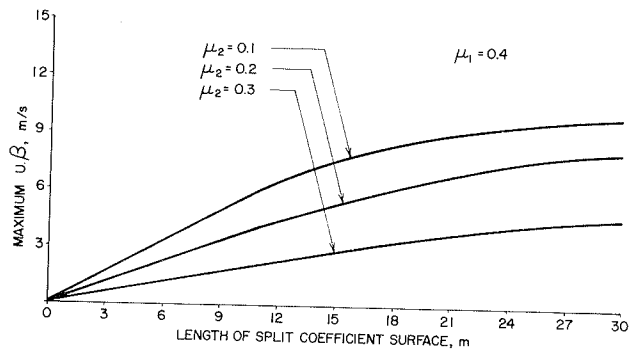

Figure 13. Recommended maximum lengths of differential friction for safe operation of cars in skidding maneuvers (vehicle speed at inception of skid = 88 km/h).

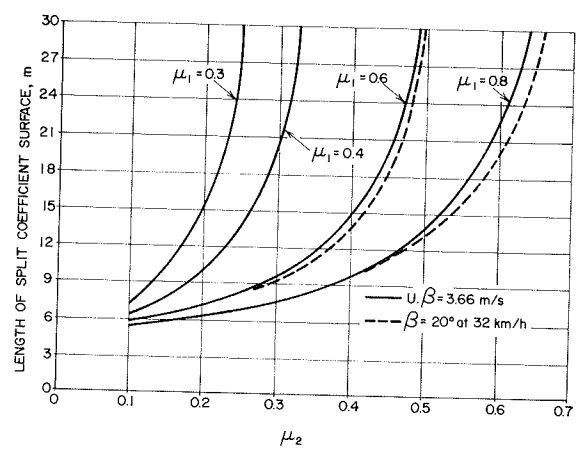

13 are curves indicating when drift angle exceeded 20° at a vehicle speed of 32 km/h. Figure 13 shows boundaries of safe operation: If a given combination of the two coefficients of friction and the length of differential-friction surface falls to the left of the appropriate curve, unsafe operation is indicated; if the combination falls to the right of the appropriate curve, safe operation is indicated.

In using Figure 13, a first estimate of the coefficients of friction may be obtained by taking values of SN_{40} measured by ASTM E274 (1) for the respective surfaces, dividing by 100, and entering directly. If it is required to account for the fact that an SN_{40} measurement [made with an ASTM E501 (1) tire] overestimates the skid resistance of a low-macrotexture surface as experienced by a worn tire, the coefficient of friction may be estimated from values of skid resistance measured with an ASTM E524 (1) blank tread tire or from macrotexture and microtexture measurements. However, skid-resistance measurements made by the ASTM E274 method (1) should be used with care. The transformation and interpretation of such measurements should be made at the discretion of the user.

CONCLUSIONS

The results presented in Figure 13 are applicable only to skidding maneuvers in which the skid was initiated by some factor other than the presence of differential friction. Maintaining the vehicle in the skid is then considered to be the safest course of action for the driver if the differential friction causes the vehicle to exceed a given value of angular deviation from the original path. The previously defined parameters of angular deviation are measures of how difficult it will be for the driver to regain control and subsequently steer the vehicle on a path within the roadway boundaries should he or she release the brakes at some point during the skid. Only tangent sections with 3.66 m of allowable lateral maneuvering space were considered, although smaller lateral distances and curved sections could also be included by changing the allowable limit of the parameter $U \cdot \beta$.

However, the extremely complex and variable nature of human behavior and a lack of experimental data make it very difficult to set numerical values for the parameter limits. This constitutes the most serious source of error (or uncertainty) in the boundaries of safe operation shown in Figure 13. Further studies of driver behavior and an analysis of accidents occurring on split-coefficient roadway surfaces are required to validate (a) the choice of parameters to indicate potential loss of control and (b) the numerical parameter values that give the boundaries of safe operation.

The chart shown in Figure 13 is therefore a first approximation of the boundaries of safe operation and should be used only as a guide. It should also be noted that a boundary of safe operation implies an acceptable level of risk rather than a definite boundary below which no accidents will occur.

Differential friction may also initiate an emergency when a vehicle is being braked, since the wheels on the low-coefficient surface may lock if the surface cannot generate sufficient tire friction force. The locking of three or fewer of the wheels will yaw the vehicle in much the same manner as will a four-wheel skid on a split-coefficient surface, except that the driver retains a measure of lateral control through the wheels that are not locked. Skidding maneuvers initiated by pavement markings may therefore not be as serious as maneuvers that result from releasing the brakes of a vehicle during a four-wheel skid. But this consideration should be weighed against the fact that the emergency has been caused by the differential friction.

Other factors that contribute to differences between the simulated trajectories from which Figure 13 was generated and the trajectory of a car on the highway involve modeling simplifications and estimation of coefficients of friction. In view of the difficulty of predicting human behavior during emergencies, improving the accuracy of modeling would probably not give a significant improvement in the degree of uncertainty associated with the use of Figure 13. Estimation of the effective coefficients of friction is a practical matter that depends on the procedure used to measure skid resistance and on the vehicle tire configuration (worn, mixed, winter tread, etc.) that is to be considered as typical or representative.

The most important factors likely to contribute to discrepancies in the simulation results are the following:

1. The vehicle parameters used in the simulation were for a full-sized sedan. Other vehicle configurations or off-design values will give different results.
2. The coefficient of friction was modeled as being independent of tire sliding speed. Low-speed skid resistance and the relation between skid resistance and speed for different tire-pavement pairs are to a large extent independent. Allowing the coefficient of friction to vary with speed would therefore have greatly increased the number of simulation runs because of the increased number of possible combinations of pavement friction coefficients.
3. The roadway was considered to be flat and horizontal. A vehicle sliding on a superelevated roadway will tend to slide laterally, and changes in grade will change the distance required for the vehicle to stop.
4. The vehicle model did not have a roll degree of freedom. Probably the most serious aspect of this restriction is that there is some evidence of coupling between vehicle roll and driver steering input, during severe maneuvers, which may lead to instability. At this time, such complications cannot be modeled.

ACKNOWLEDGMENT

The research described in this paper was developed from work conducted as part of a Federal Highway Administration research project. Edward Harrigan served as technical monitor of this project, and his assistance is greatly appreciated.

REFERENCES

1. Annual Book of ASTM Standards. ASTM, Philadelphia, Part 15, 1980.
2. H. Dugoff, P.S. Fancher, and L. Segel. An Analysis of Tire Traction Properties and Their Influence on Vehicle Dynamic Performance. Trans., SAE, Vol. 79, Paper 700 377, 1970.
3. W. Lincke, B. Richter, and R. Schmidt. Simulations and Measurement of Driver Vehicle Handling Response. SAE, Warrendale, PA, Paper 730 489, 1973.
4. J.C. Burns. Differential Friction: A Potential Skid Hazard. TRB, Transportation Research Record 602, 1977, pp. 46-53.
5. W. Zuk. The Dynamics of Vehicle Skid Deviation as Caused by Road Condition. Virginia Council of Highway Investigation and Research, Charlottesville, June 1958.
6. G.F. Hayhoe. A Driver Model Based on the Cerebellar Model Articulation Controller. Vehicle

System Dynamics, Vol. 8, 1979, pp. 49-72.
7. D.T. McRuer and R.H. Klein. Automobile Controllability: Driver/Vehicle Response for Steering Control: Volume 1--Summary Report. U.S. Department of Transportation, Rept. TR-1040-1-I, 1975, 269 pp. NTIS: PB 240 208.

Publication of this paper sponsored by Committee on Surface Properties-Vehicle Interaction.

Groove-Depth Requirements for Tine-Textured Pavements

JOHN E. GRADY AND WILLIAM P. CHAMBERLIN

This paper discusses the depth required for grooves on new tine-textured concrete pavements in order to ensure an adequate skid resistance over their entire design life. It is based on measures of texture depth and skid resistance, with both ribbed and smooth tires, made on new to 5-year-old pavements in New York. Initial groove-depth needs of 3/16-in minimum were calculated from two values estimated from the study data: (a) minimum groove depth (0.050 in) to ensure adequate skid resistance with a minimum legal tire tread and (b) mean groove wear rate (0.013 in/million vehicle passes). Groove depth measurements on new concrete pavements and bridge decks indicated 21 and 14 percent compliance, respectively, with the proposed new standard of 3/16-in minimum, and 60 and 44 percent compliance with the current standard of 2/16-in minimum. Prospects for improving the compliance rate were judged to be most promising in two areas—increasing the awareness and motivation of construction personnel and improving the design of tining rakes over those now in use. Although the findings of this study are specific to standards and conditions in New York, the methodology should be of general interest.

Many highway agencies require a tined finish on new portland cement concrete pavements (1). The method was introduced because textures obtained by previous methods were found to wear too quickly, and pavements provided only marginal skid resistance after passage of a relatively few vehicles (2). Although assumptions of improved durability and skid resistance over other methods have been generally confirmed (3), the relative newness of tine texturing has precluded evaluation of its long-term durability and skid resistance under actual traffic. Ensurance of adequate skid resistance over a pavement's entire design life requires knowledge of minimum texture needs and the rate at which texture and skid resistance decay, so that the depth of groove required at construction can be judged. This paper describes the collection and analysis of data to address these questions. Although the findings reflect specific needs and conditions in New York State, the methodology is generally applicable.

PURPOSE AND SCOPE

The primary purpose of the study was to determine the rate at which tined textures, and the skid resistance they provide, decay under traffic, and thus to determine what initial groove depth is required to sustain adequate skid resistance over a pavement's entire design life. A related consideration was that an evaluation of the effectiveness of current design practices, including skid-resistance-decay rates, had been recommended by the Federal Highway Administration (FHWA) (4), though this policy is under review (5).

A secondary purpose was to evaluate newly constructed pavements and bridge decks for compliance with specified texture depth. New York requires a groove depth of 3/16 ± 1/16 in (6), but past experience has shown that texture depths vary significantly from job to job, and even within the same job (7). It was believed that data collected on new construction would show whether depths actually obtained are sufficient to permit adequate skid resistance over the entire design life, given the decay rate measured.

The study was based on measures of skid resistance and texture parameters collected in 1978 and 1979 on 11 in-service pavements, 9 unopened pavements, and 25 unopened bridge decks. These sites represented all of those that, by the summer of 1978, had been finished with a tined texture under new specifications implemented in 1974. In all cases, pavements were built with a New York State class C concrete mix (nominal water-cement ratio = 0.44, cement factor = 6.4), and bridge decks were built with a class E mix (nominal water-cement ratio = 0.44, cement factor = 7.0).

PROCEDURES AND RESULTS

Texture wear rates were estimated from texture depth measurements and ribbed-tire skid resistance tests on 11 pavements in service (series 1). To extend the range of corresponding traffic volumes, measurements were made in both the driving and passing lanes and for two years (1978 and 1979). Five sites were tested in each lane of each pavement, for a total of 110 sites.

The minimum mean groove depth (MGD) required to provide adequate drainage beneath a minimum legal tire tread (2/32 in deep in New York) was estimated from texture and skid resistance measurements with both ribbed and smooth tires at 30 additional sites, selected from these same 11 pavements (series 2). These additional sites were chosen to represent as wide a range in groove depth among sites as possible and also because each was relatively uniform within the distance required for a valid skid test--about 60 ft.

To judge compliance with the current specification as well as with initial texture depth needs determined from this study, depths were also measured on 9 unopened pavements and 25 unopened bridge decks (series 3). The entire testing program is outlined in the table below.

Variable	Series 1	Series 2	Series 3
Objective	Wear rates	Groove depth	Compliance
Test pavements	11	4	9, including 25 bridge decks